
Duty-Based Dumping Control for Underground Load-Haul-Dump Vehicle Based on Reinforcement Learning

LuLu Gao ^{1,*}, Zihang Zhang¹, Johannes Sprink², Katharina Schmitz²

¹ School of Mechanical Engineering, University of Science & Technology Beijing, Beijing, 100083, China

² ifas, RWTH Aachen University, Campus-Boulevard 30, 52074 Aachen, Germany

* Corresponding author: Tel.: +86-15201463530; E-mail address: gaolulu@ustb.edu.cn

Abstract.

Underground load-haul-dump (LHD) vehicles, with the excellent maneuverability and efficiency, are widely used to the materials removal in underground mines and constructions. Owing to the harsh operation environment, the autonomous functions of LHDs have been urgently needed for the consideration of safety, efficiency, and cost. Dumping is one of the core functions for underground load-haul-dump (LHD) vehicles. Typical underground environment including narrow space and varying dumping locations restricted the unconstrained autonomous dumping. This paper probes into the autonomous dumping control of LHDs under narrow and constrained environment based on the reinforcement learning (RL) frame. Firstly, the kinematic and dynamic models of a LHD are established considering the data-dependency of the RL method. The duty-based RL control method, is proposed to realize the coordinative control of the driving system and the working system in dumping duty, in which the safety in avoiding collision and working efficiency were considered. A test platform was established with the LHD to validate the methods. For the RL-based method, the performance of different algorithms was evaluated. A typical dump duty was performed to validate the method. The results shown that the method could finish the dumping operation autonomously under constrained environment. The duty-based RL control method shown great coordinative characteristics and environmental adaptability with the RL frame under constrained environment.

Keywords. Underground load-haul-dump (LHD), Dumping operation, reinforcement learning (RL), Duty-based, Coordinative

1. INTRODUCTION

Underground load-haul-dump (LHD) vehicles are essential equipment in underground mining and construction due to the excellent maneuverability and operational efficiency[1-2]. However, the harsh and confined working conditions pose significant challenges to automation, driving an urgent need for autonomous LHDs functionalities to enhance safety, productivity, and cost-effectiveness. The autonomous operations of LHDs evolve through five stages: driver-only, assisted, semi-autonomous, highly-autonomous, and fully autonomous, with current operations transitioning from assisted to semi-autonomous[3].

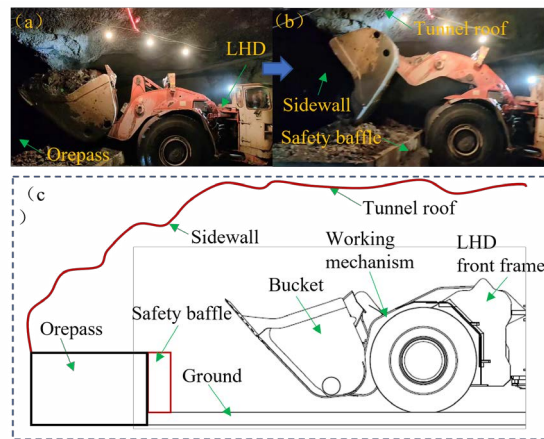


Figure 1: Typical dumping environment of underground LHD

The working environment of LHDs is narrow and constrained, as shown in Fig. 1, which functions include loading, hauling, and dumping materials. The autonomous loading function has been focused for many years considering the decisive effect on working efficiency. However, the interaction between materials and bucket is complex and the characteristics of materials varies significantly[4], which blocked the practical application and made the autonomous loading challenging and long term developing-needed. The autonomous hauling can be realized with the trajectory tracking of articulated vehicles, which has been applied in the practical working process. The dumping operation, one of the core function of LHDs, involved the control of the driving system and the working mechanism. Although the operation could be performed with the pre-set automation program, the driving system and working mechanism were not controlled coordinately as manual control. Current autonomous dumping would be inefficiency and unsafe in constrained environment. In addition, the variation of dump point and environment constraints could not be covered. Therefore, the improvement of autonomous dumping function would be practical and effective for the autonomous development transition[5-6].

The dumping function of LHDs could be realized with the pose (including trajectory and attitude angle) control of bucket. For the pose control, the traditional proportional-integral-derivative (PID) method would be the first choice considering the simple structure and stable performance. There are two problems to be addressed before the application of PID. First, the target/reference values of the controlled lift, dump cylinders, and the driving system should be provided via the inverse kinematics of the vehicle and the working mechanism.

The kinematics of the six link mechanism provided a feasible solution obtained from cumbersome calculation. Second, the parameters of PID must be tuned individually. Different algorithms had been used to tune the parameters, such as fuzzy logic, neural network (NN), and genetic algorithm (GA). Some modern control methods were also used to the trajectory tracking of bucket, including mode predictive control (MPC), optimal control, and RL-based methods[7-9]. However, most of these researches studied the trajectory control of bucket in open area and unconstrained environment, or only the working mechanism of LHDs[10] was mainly focused.

Inspired by the aforementioned researches, this paper explores the duty-based RL autonomous dumping control method. First, the models of the LHD and the corresponding test platform are established considering the data-dependency of the RL methods. Then, the duty-based RL control method (DRLC) is proposed with the RL frame, in which the completion rate, working efficiency, and environment constrains are covered. The performance of different algorithms and preview horizon in the methods, including deep deterministic policy gradient (DDPG), twin Delayed Deep Deterministic policy gradient algorithm(TD3), SAC, and distributional SAC (DSAC)[11], are evaluated under typical dumping operation. The main contributions of this paper include: (1) An environment-adapted control method for autonomous dumping of LHDs is established based on the RL frame; (2) The performance of different algorithms and preview horizon are uncovered under typical dumping operations; (3) The performance of RL-based methods is evaluated in terms of safety and efficiency.

2. KINEMATIC AND DYNAMIC MODEL

The working mechanism of the LHD is a typical reverse Z-shape six link mechanism, as shown in Fig. 2, the actuators of the whole system are the lift and dump cylinders. During the lifting process, if only the lift cylinder is controlled, the angle of bucket would vary, which would lead the scattering of the ore materials. Therefore, the whole autonomous dumping operation in constrained environment can only be realized with the coordinate control of the driving system and the working mechanism.

2.1. Model of LHD

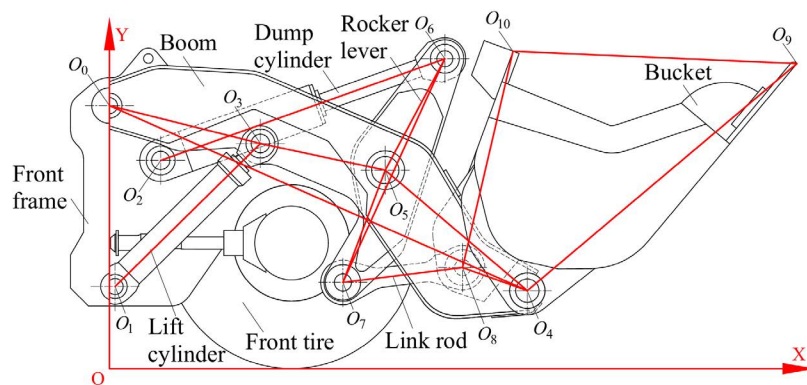


Figure 2: Working mechanism of LHD

The kinematic model of LHD and the working mechanism are involved during the dumping operation control. For working mechanism, as shown in Fig. 2, the boom is connected with the front frame (at O_0), rocker lever (at O_5), bucket (at O_4), and the lift cylinder (at O_3). The two connecting points of cylinders are O_1 and O_2 , respectively. The motion of the working mechanism can be described in the coordinate frame (XOY), in which the vertical direction across the O_0 is defined as Y axis, and the horizontal tangent direction of front tire is defined as X axis.

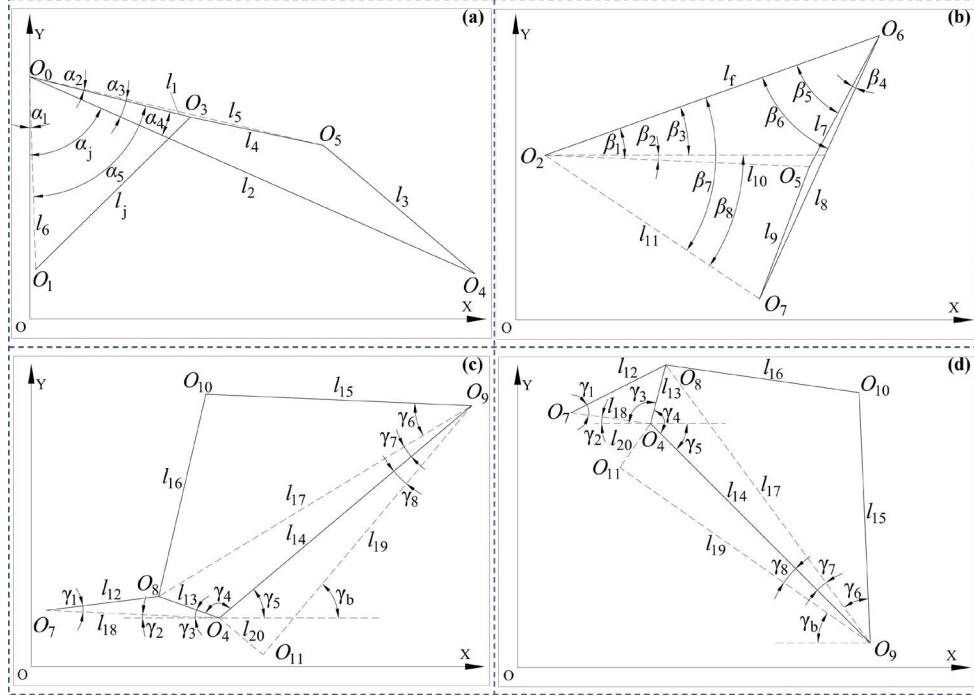


Figure 3: Geometric relationship of different states of working mechanism

The geometric relationship of bucket in dumping state is shown in Fig. 3 (d), and the coordinate of bucket tip O_9 can be expressed as:

$$\begin{cases} X_9 = X_4 + l_{14} \cos \gamma_5 \\ Y_9 = Y_4 + l_{14} \sin \gamma_5 \\ X_{10} = X_9 - l_{15} \cos(\gamma_6 + \gamma_7 - \gamma_5) \\ Y_{10} = Y_9 + l_{15} \sin(\gamma_6 + \gamma_7 - \gamma_5) \end{cases} \quad (1)$$

in which γ_b is the angle between bucket bottom and horizontal direction., the forward kinematics of the working mechanism can be obtained with the related geometry relationship in Figure 3.

Considering that the dumping operation is finished with driving system and working mechanism (no steering maneuver is involved), the longitudinal dynamic model of the LHD should be established. The longitudinal dynamic model of LHD in the X axis of global coordinate frame can be described as:

$$m\ddot{x} = F_{tx} - F_r \quad (2)$$

in which, m is the mass of LHD, F_{tx} , F_r are the longitudinal driving force, and total resistance force, respectively, x is the longitudinal distance of LHD in global coordinate frame.

The longitudinal force of tires can be given by Magic Formula:

$$F_{tx} = S_y + D \sin \left\{ C \arctan \left[\begin{array}{l} B(X_m - S_x)(1 - E) \\ + E \arctan B(X_m - S_x) \end{array} \right] \right\} \quad (3)$$

where X_m denotes the slip ratio of the tire, which are defined as η ; F_{tx} denotes the longitudinal force of tire; the parameters S_x , S_y , B , C , D , and E are constant, where in this study $S_x = 0$, $S_y = 0$, and other parameters are calculated by equations with vertical load. The slip ratio of different tire can be given by:

$$\eta = \begin{cases} (r_d \omega_t - v_x) / r_d \omega_t \times 100\% & \text{Drive} \\ (r_d \omega_t - v_x) / v_x \times 100\% & \text{Brake} \end{cases} \quad (4)$$

where r_d denotes the rolling radius of different tires, ω_t denotes the angular velocity of tires, and v_x denotes the longitudinal velocity of LHD. The final drive torque in the wheel overcomes the rolling resistance force and braking force to produce the longitudinal driving force, and the detailed model can be expressed as:

$$I_w \dot{\omega}_t = T_d - f_r - F_{tz} r_d - F_{tx} r_d \quad (5)$$

where I_w is the rotational inertia of the wheel, and T_d is the driving torque, F_{tz} is the vertical load of tires. f_r is the rolling resistance force, which can be expressed as:

$$\begin{cases} f_r = 0.00792 + 0.00025 v_x & v_x \neq 0 \\ f_r = 0 & v_x = 0 \end{cases} \quad (6)$$

The longitudinal dynamic model of LHD can be obtained by combing equation (2) - (6). Therefore, the bucket pose in global frame could be given by combing the kinematic and dynamic models:

$$\begin{cases} X_{11} = x + X_4 + l_{14} \cos \gamma_5 \\ Y_{11} = y + Y_4 + l_{14} \cos \gamma_5 \end{cases} \quad (7)$$

where X_{11} , Y_{11} are the coordinates of bucket tip O_9 in global frame. y is the vertical distance of local and global frames.

2.2. Model validation

To validate the involved models, an LHD test system is established, as shown in Fig. 4. The control system is a two-layer structure system, in which an industrial computer is used in the upper layer for the functions of perception, navigation, and control decision. A 16 line LiDAR and inertial measurement unit (IMU) are used to obtain the vehicle state and the operation environment in the test site. The control target of the driving system and the working mechanism, including the velocity of LHD, angle of boom and displacement of dump cylinders, are given to the lower controller, including five EPEC controllers. The EPEC controllers are used to control the longitudinal velocity and the hydraulic related actuators, including steering, lift, and dump cylinders. Only the control of the driving system and the working mechanism during dumping operation are considered in this paper considering that the steering system is not involved during the late stage of dump operation. A displacement sensor is used to obtain the displacement of dump cylinder. For pressure sensors are used to record the pressure data of the two

cylinders during operations. Two angle sensors are used to measure the angle of boom and the spatial angle state of bucket. In addition, a revolution sensor is used to obtain the rotation speed of front tire, i.e., the longitudinal velocity of LHD. The controllers can communicate with each other via CAN bus. The details of the involved devices are shown in Tab. 1.

Table 1: Detail parameters of the devices

Device	Parameters
Industrial computer	Nvidia jetson agx Xavier
IMU	XW-GI5610
LiDAR	LSLIDAR C16
Displacement sensor	BTL6, 0~10V, 0~1000mm
Angle sensor	SVCK15, $\pm 180^\circ$
Revolution sensor	HC3806-1024, 12V
Pressure sensor	SUP-P300, 0-30MPa
EPEC controller	EPEC 3724

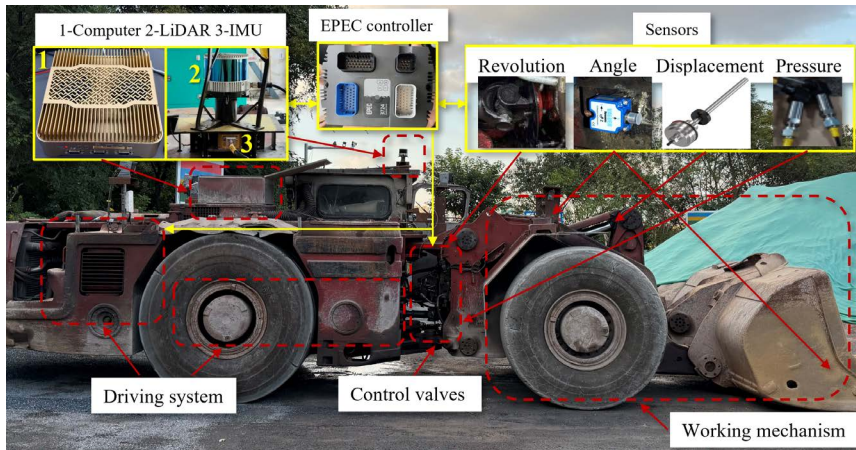


Figure 4: Schematic of test system

The dynamic model of LHD and kinematic model of the working mechanism were validated, separately. For the validation of longitudinal dynamic model, same control signal of driving system was used in the model simulation and field test, and the responses of longitudinal velocity and position were compared in Fig. 5. The longitudinal velocity of test and simulation results coincided well during the test interval, and only minor differences appeared during the free-running period, i.e., 39~41.8 s and 9.2~10.1 s. This error was brought on by the rolling resistance force model. The used resistance force model was established based on the paved road condition, while the test road was an unpaved road. The maximum velocity of the test was about 7.1 km/h, and the corresponding result was about 6.9 km/h. Fig. 5 (b) shown the position result of test and simulation. As it can be seen, the longitudinal position was about 26.4 m, and the next stop position was about 52.6 m. The simulation results given the 25.3 m and 52.1 m. It meant that the maximum position error was less than 4.2 %. These results indicated that the established dynamic model could reveal the dynamic characteristics of LHD in longitudinal direction.

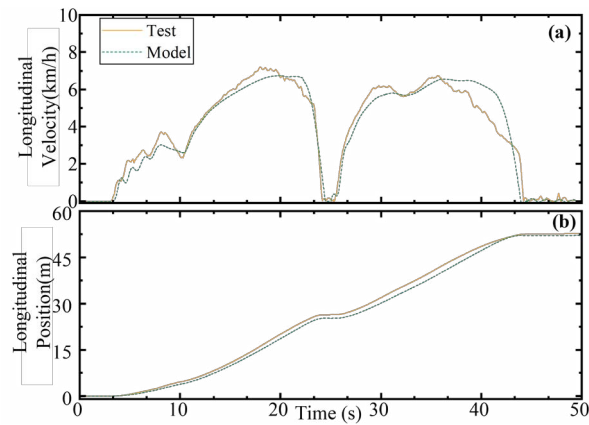


Figure 5: Comparing results of longitudinal dynamic model validation

For the validation of working mechanism, the displacement of cylinder and angle of boom and bucket were recorded. And the coordinate of bucket tip point O_9 was manually measured. Then the displacement results and angle results were input into the forward kinematic model, and the results of bucket angle and coordinate of bucket tip point were obtained continuously as the simulation results. According to the results in Fig. 6 (a)(b), the displacement of dump cylinder varied between 1256.8 – 1852.8 mm and the angle of boom varied between 65.3° - 109.4° . The comparing results of bucket tip position was shown in Fig. 6 (c), in which nine scatter coordinates are the actual measured values. The detailed values of bucket tip position were compared in Tab. II. The average error in Y-axis was larger than the error in X-axis, and the average error rate was about 0.2% and 0.5% in X and Y directions, respectively. The angle of bucket varied between -59.8° - 46.2° according to Fig. 6 (d). The maximum angle error was about 1.4° , at about 36 s. The error rate of angle was about 1.1%. These results indicated that the kinematic model was accurate enough for the research of dumping control.

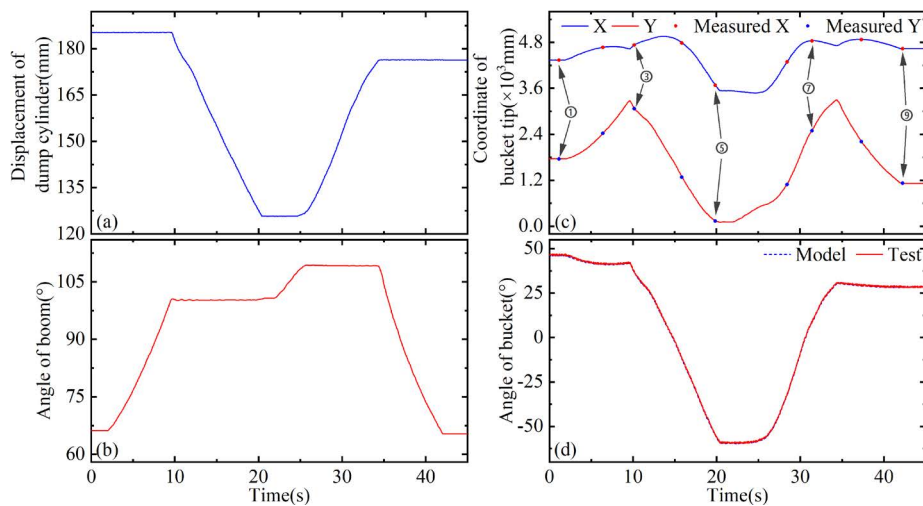


Figure 6: Comparing results of kinematic model validation

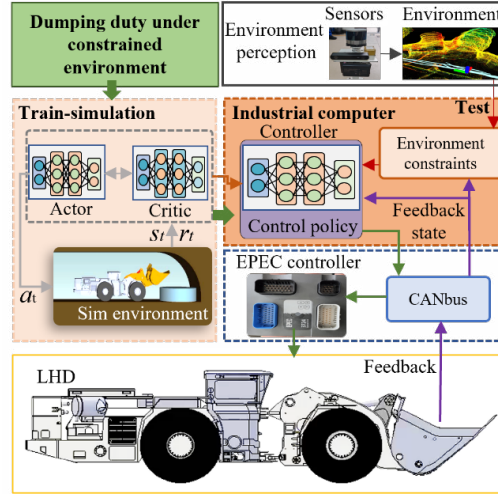
Table 2: Detail values of bucket tip position

	Model(mm)	Measured(mm)	Error(mm)
1	x=4343.6, y=1757.0	x=4336.9, y=1761.7	ex=6.7, ey=4.7
2	x=4669.3, y=2418.5	x=4664.7, y=2413.3	ex=4.6, ey=5.2
3	x=4732.0, y=3077.8	x=4728.2, y=3088.9	ex=3.8, ey=11.1
4	x=4788.9, y=1291.9	x=4782.7, y=1300.3	ex=6.2, ey=8.4
5	x=3686.0, y=150.4	x=3679.2, y=157.6	ex=6.8, ey=7.2
6	x=4291.3, y=1105.0	x=4283.7, y=1114.7	ex=7.6, ey=9.7
7	x=4841.0, y=2504.9	x=4832.2, y=2521.1	ex=8.8, ey=16.2
8	x=4876.7, y=2210.8	x=4870.4, y=2221.3	ex=6.3, ey=10.5
9	x=4632.9, y=1117.3	x=4628.7, y=1113.2	ex=4.2, ey=4.1

Based on the above analysis results, it can be concluded that the established dynamic and kinematic models could reveal the characteristic of driving system and working mechanism during dumping operation. And the models were accurate enough for the RL-related method.

3. AUTONOMOUS DUMPING CONTROL METHODS

The RL frame was used to realize the coordinate control of the driving and the working system in this section. During the manual operation, the operator can freely perform the control according to current states and target duty until the required duty is completed. Therefore, we designed the duty-based RL control method (DRLC), the duty-driven characteristics of manual operation is considered.

**Figure 7:** Schematic of RL-based dump control method

As stated before, the LHD is operated in narrow underground mine. The excellent efficiency of manual LHD originates from the preview characteristic of operators. It means that the operator could see the target ore pile, path, and ore pass in advance. Reasonable operation for driving system and working mechanism could be implemented according to the current states of LHD and the information of duty and

environment. Inspired by this characteristic, the DRLC is designed in this section. We designed an autonomous dump system for LHD based on the RL frame in this section to improve the efficiency and safety, as shown in Fig. 7.

For the whole system, the environment information, including the position of ore pass, tunnel, safety baffle, and LHD, were obtained with related sensors, as stated in test system. The environment constraints, including the tunnel roof, side wall, and safety baffle, are extracted. The trained control policy with RL frame in the controller gives the target trajectory of bucket point considering the collision risk, states and actuator constraints of LHD and further specifies the actuator targets of EPEC controllers, as shown in Fig. 7. The target trajectory contains the attitude angle of bucket, and X and Y location in global frame. Special attention is spent on the design of policy training based on RL.

The RL-based controller is a trained policy in essence based the RL train frame. The policy can give the control signals according to the feedback states, defined in s_t . The collision constraints during dumping operation is shown in Fig. 8. As it can be seen, the whole situation is simplified as the plane view. It means that the longitudinal symmetry line of LHD coincides with the symmetry line of the circular ore pass. The tunnel roof, sidewall, and front tire are denoted as T_1 , W_1 , and S_1 , respectively. The outline of bucket is marked as $O_4'O_9O_{10}O_8'$. The outline of safety baffle is marked as B_1 . For the ore pass, the out point is marked as P_1 , and the inner points are marked as P_2 and P_3 , respectively. The lower point of boom is marked as L_1 .

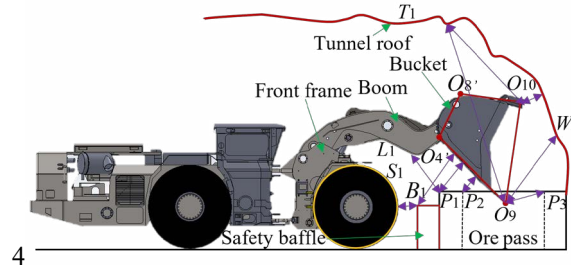


Figure 8: Collision constraints during dumping operation.

For the safety baffle, the collision, with front tire S_1 , lower point of boom L_1 , and bucket $O_4'O_9O_{10}O_8'$, might occur. For ore pass, the collision might occur between ore pass, low point of boom, and bucket. As it can be seen from Fig. 8, although the outline of bucket and ore pass is intersecting, no collision occur. It means that the middle channel of ore pass is free for bucket. For the main moving parts, the collision might occur between bucket and tunnel roof, bucket and sidewall of tunnel. All of the safety constraints is expressed as:

$$C = S(g(f_1, f_2)) \quad (8)$$

in which C is the collision results, it has two values, i.e., 1 and 0. The value 1 denotes the collision occurs, and the value 0 denotes the motion of LHD is free to collision. $g(\cdot)$ is the closest distance calculation function. f_1 contains $O_4'O_9O_{10}O_8'$, S_1 , and L_1 , f_2 contains T_1 , W_1 , B_1 , and $P_1 - P_3$. $S(\cdot)$ is specified as:

$$S(x) = \begin{cases} 1 & x \leq x_{lim} \\ 0 & x > x_{lim} \end{cases} \quad (9)$$

in which x_{lim} is the threshold for collision detection. Then the collision reward could be given by:

$$r_c = -c_6 C \quad (10)$$

4. RESULTS AND DISCUSSION

4.1. Simulation validation of ADC

A dumping operation is performed firstly in simulation environment to validate DRLC. The control policy was obtained with DSAC algorithm. The dump operation scene is concretized, as shown in Fig. 9. As it can be seen, the ore pass is concretized as a hollow cylinder with a height of 0.8 m, an inner diameter of 2.8 m, and an outer diameter of 1 m. The safety baffle is a rectangular prism with a section height of 0.6 m and a width of 0.4 m. The distance between the center of the front wheel and the center of the ore pass is 22.0 m. The distance between the center of the front wheel and the left side of safety baffle is 20.0 m. The motion of bucket is constrained with 3.8 m in the top direction, which is the distance between the tunnel roof and front wheel center. The side wall around ore pass is simplified as a circular arc with 3.0 m radius.

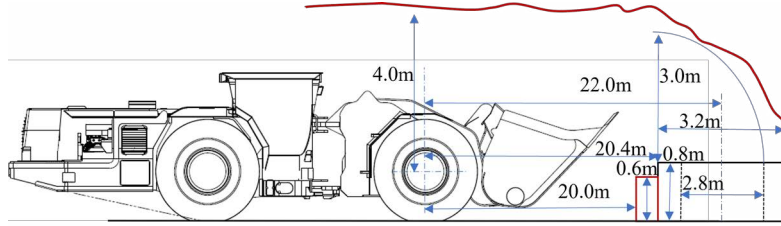


Figure 9: A typical dumping scene in constraint environment

The results of DRLC are shown in Fig. 10 - Fig. 11. The state results of bucket tip were shown in Fig. 10, in which the subfigures (a), (b), and (c) are the results of displacement in X direction, in Y direction, and attitude angle, respectively.

As it can be seen from Fig. 10 (a), the LHD was planned to run longitudinally from start point 0 m to final point 21.9 m. The control result coincided well reaching the target location. The front point of bucket was within the range of ore pass, which is very important for the dumping operation. As it can be seen from Fig. 10 (b), the vertical direction distance, i.e. the Y axis was planned to lift from 1.74 m to 3.19 m, and then fallen from 3.19 m to 0.72 m. The motion of simulation coincided well avoiding obstacles and reaching the target location. For the attitude angle of bucket, i.e., γ , shown in Fig. 10 (c). The angle varied slightly during the lifting stage. The variation was about 5.4° , during 40.8° and 46.2° , which made sure there was no scattering dumping the lifting stage. Then bucket was operated to tilt during 21 s - 29 s. The final tilt angle was about -54.2° .

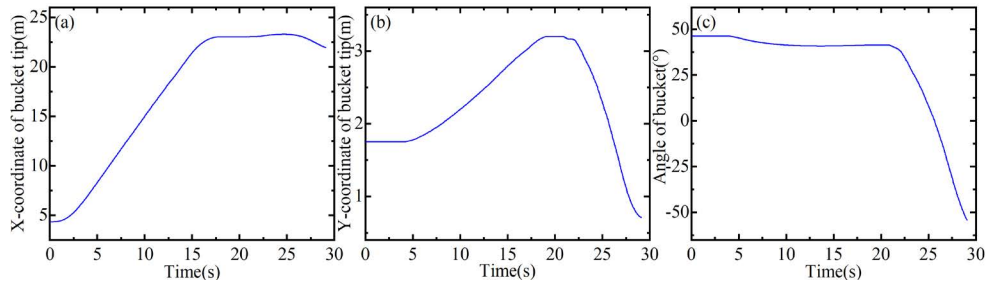


Figure 10: Simulation results of displacement and angle in dump operation.

In order to analyze the dumping operation, the trajectories of bucket tip and front tire were recorded in Fig. 11. The location of ore pass and safety baffle was also indicated in the figure. As it can be seen, the DRLC can control the trajectory of bucket front tip to finish dumping operation. The final operation was finished within the range of ore pass. In addition, the LHD stop in front of safety baffle with an appropriate distance according the results of tire trajectory. Based on the above analysis, it can be concluded that the DRLC can control LHD to finish dump operation autonomously and precisely.

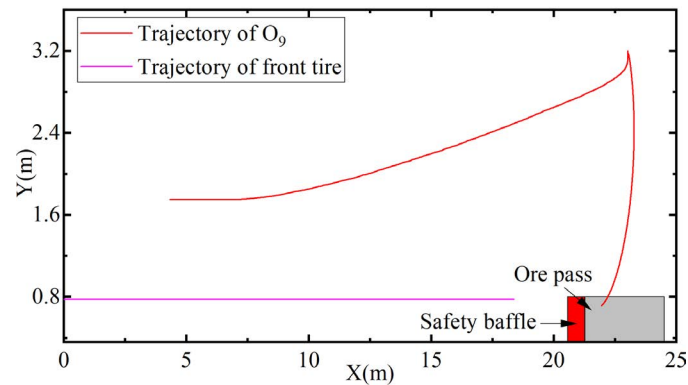


Figure 11: Bucket tip trajectory results of RLPC

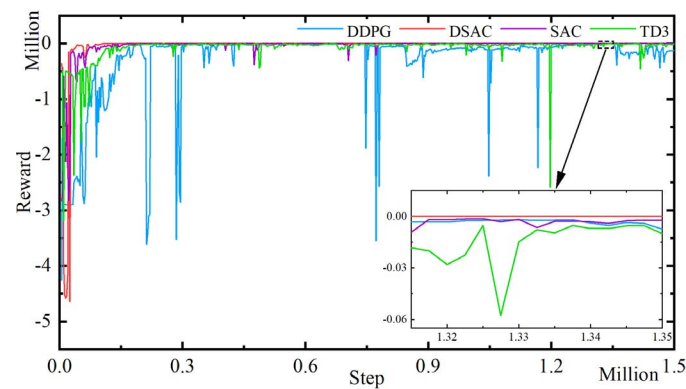


Figure 12: Reward results of different algorithm.

In order to explore the performances of different RL algorithms, trains of different algorithms, including DDPG, TD3, SAC, and DSAC, were performed based on the same dump operation and RLPC. For the train process, the same environment was used, and same values were used for the same parameters.

The reward of different algorithms was shown in Fig. 12. The maximum train step is 1.5 million. As it can be seen, DSAC and SAC show a faster increase trend at the start stage, and the TD3 is also fast than DDPG. The DSAC and SAC also show a more stable increase trend during the middle stage. In addition, the detailed figure also indicated that the DSAC shown higher reward during the whole process, which indicated that it given better comprehensive performance during the dumping operations.

4.2. Test results and discussion

In order to validate the proposed methods further, the test of dumping operation was performed with the aforementioned test platform. The system was implemented with the control policy trained with DSAC. The velocity and longitudinal location results were shown in Fig. 13 (a) and (b), in which the output of RL controller was marked as “Sim”, and the actual results of LHD was marked as “Test”.

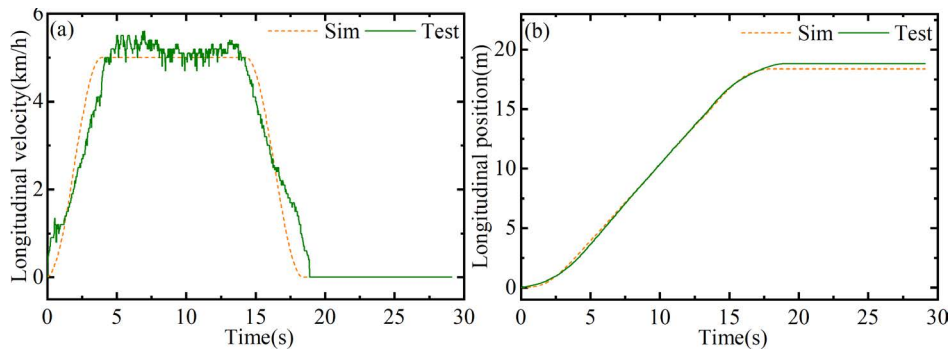


Figure 13: Velocity and longitudinal distance test results of RL-based method.

As it can be seen, the proposed method could control LHD run to target ore pass location. The max deviation during running process was about 0.2 m. The last stop point in the test was about 20.0 m. The error of longitudinal control was less than 1.2%. It was less than the error threshold for engineering application, i.e., 5%. The fluctuation of the velocity aroused during the acceleration and deceleration phases, as shown in Fig. 13. The actual velocity results indicated that the proposed method could guarantee LHD run as expected, although more fluctuation occurred in the actual velocity result. The maximum velocity error was about 0.33 m/s. The longitudinal result validated the drive system control performance of the proposed method.

The results of lift and dump cylinder displacement, and the attitude angle of bucket, γ , are shown in Fig. 14. As it can be seen, the dump cylinder kept static during the driving stage, 0 - 20 s. The displacement of dump cylinder at this stage was about 184.3 cm. The attitude angle of bucket varied slightly during 44.5° and 39.8° and the variation was about 4.7° . The lift operation started at 4.0 s, the LHD was still run with the 5.0 km/h velocity. The dump operation was performed at 21.4 s after the LHD stopped and

the lift cylinder arrived at the target displacement. The results of boom angle shown that the lift and dump cylinder were controlled coordinately between 21.4s to 29.1s. The range of boom angle varies from 100.0° to 111.3° , while the displacement of dump cylinder changed between 184.3 cm to 130.7 cm. The final attitude angle was about -52.1° , which guarantee the dump of ore materials. Therefore, it can be concluded that the proposed method, DRLC, could finish the dump operation autonomously and coordinately.

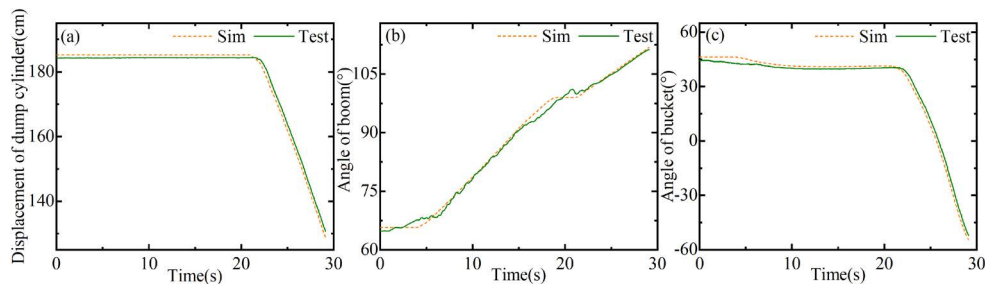


Figure 14: Cylinder displacement test results of RL-based method.

In order to further analyze the dump operation during test, the trajectory of bucket tip in the LHD frame is shown in Fig. 15. As it can be seen, the start and stop point of test and reference almost coincided with each other, although the difference occurred during the internal process. The final resulting bucket tip position was about 22.5 m in longitudinal direction, and 0.52 m in vertical direction. Therefore, it can be concluded that the proposed method could control the bucket to finish the dump operation safety. The whole dump operation was finished within 29.1 s according to the results.

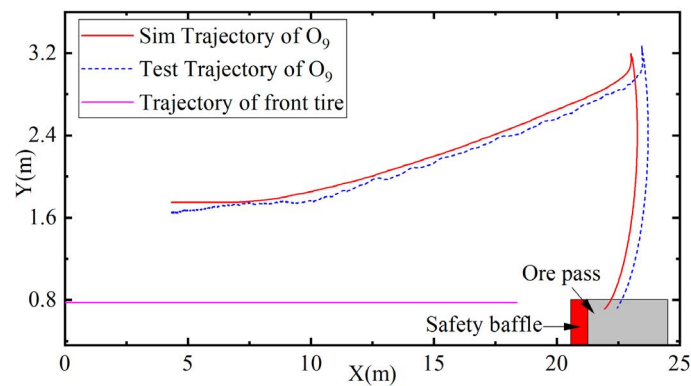


Figure 15: Trajectory of bucket tip in test.

Based on the above results, the proposed method in this paper could finish the dump operation with 29.1 s. The coordinate control in the proposed method guarantee the better state of bucket in lift process. The variation of attitude angle was about 5° , and meet the error threshold for engineering application. The less variation meant that less ore materials was scattered during lift process. The appropriate stop point result also indicates that the method could guarantee collision safety during the dump motion.

Therefore, it could be concluded that the method could finish dump operation with excellent safety, efficiency, and environmental adaptability.

5. CONCLUSION

This paper proposed an autonomous dump control method based RL frame for LHD under constrained environment. The involved dynamic and kinematic model during dump operation were established and validated with a LHD test platform. The kinematic model errors in terms of longitudinal, vertical position, and attitude angle were 0.2%, 0.5%, and 1.1%, respectively, and the longitudinal dynamic model error was about 4.2 %. The corresponding design details about the duty-based method (DRLC) was presented, in which the constraints of driving system and working mechanism actuators, and collision safety were considered, while also accounting for the completion status of the dumping operation. The effect of different RL algorithms was explored for dump occasion, in which the DSAC shown better performance. The field tests of autonomous dump operation with DRLC was performed. The results shown that the proposed method could finish the dump operation with 29.1 s under the premise of ensuring safety and efficiency. Therefore, the proposed method could finish dump operation with excellent safety, efficiency, and environmental adaptability.

6. REFERENCES

- [1] D. Cardenas, P. Loncomilla, F. Inostroza, I. Parra-Tsunekawa, J. Ruiz-del-Solar, Autonomous detection and loading of ore piles with load-haul-dump machines in Room & Pillar mines, *J. F. Robot.* 40 (2023) 1424–1443.
- [2] S. Dadhich, F. Sandin, U. Bodin, U. Andersson, T. Martinsson, Field test of neural-network based automatic bucket-filling algorithm for wheel-loaders, *Autom. Constr.* 97 (2019) 1–12.
- [3] C. Borngrund, F. Sandin, U. Bodin, Deep-learning-based vision for earth-moving automation, *Autom. Constr.* 133 (2022) 104013.
- [4] R. Hoeger, H. Zeng, A. Hoess, HAVEit: The future of driving. Final Report., (Deliverable D61.1) (2011) 358.
- [5] A. Hemami, F. Hassani, An Overview of Autonomous Loading of Bulk Material An Overview of Autonomous Loading of Bulk Material, (2015).
- [6] R. Filla, M. Obermayr, B. Frank, A study to compare trajectory generation algorithms for automatic bucket filling in wheel loaders, 3rd Commer. Veh. Technol. Symp. (2014) 588–605.
- [7] Y. Meng, H. Fang, G. Liang, Q. Gu, L. Liu, Bucket trajectory optimization under the automatic scooping of LHD, *Energies* 12 (2019) 1–18.
- [8] K.M. Elbayomy, Z. Jiao, H. Zhang, PID controller optimization by GA and its performances on the electro-hydraulic servo control system, *Chinese J. Aeronaut.* 21 (2008) 378–384.
- [9] R. Song, Z. Ye, L. Wang, T. He, L. Zhang, Autonomous Wheel Loader Trajectory Tracking Control Using, 2022 Am. Control Conf. (2022) 2063–2069.
- [10] D. Eriksson, R. Ghabcheloo, Comparison of machine learning methods for automatic bucket filling: An imitation learning approach, *Autom. Constr.* 150 (2023) 104843.
- [11] J. Duan, Y. Guan, S.E. Li, Y. Ren, Q. Sun, B. Cheng, Distributional Soft Actor-Critic:

Off-Policy Reinforcement Learning for Addressing Value Estimation Errors, IEEE Trans. Neural Networks Learn. Syst. 33 (2022) 6584–6598.

Biographies



Lulu Gao received the B.Tech. and Ph.D. degree in school of mechanical engineering from University of Science and Technology Beijing, Beijing, China, in 2014 and 2021. From February 2021 to July 2023, he was a postdoctoral with the school of mechanical engineering from University of Science and Technology Beijing. His current research interests include motion control of hydraulic power system, reinforcement learning application, intelligent mining heavy-duty vehicles.



Zihang Zhang received the bachelor's degree in vehicle engineering, in 2022, from the University of Science and Technology Beijing, where he is currently working toward the master's degree in vehicle engineering. His research areas include control of underground Load-Haul-Dump vehicle working mechanisms, simulation of hydraulic power systems, and reinforcement learning.



Prof. **Katharina Schmitz** studied mechanical and chemical engineering at RWTH Aachen University and Carnegie Mellon University, Pittsburgh (USA) and graduated 2015 as Dr.-Ing. at RWTH Aachen University. Since 2018, she is full professor at RWTH Aachen University and director of the Institute for Fluid Power Drives and Systems (ifas). In addition, she is Vice Dean of the Faculty for Mechanical Engineering at RWTH Aachen, a position she holds since 2020. Prof. Schmitz's awards and honors include several best paper awards and 2023 IMechE Joseph Bramah Medal award.